Volume 9, Issue 4
August 2020

ITEE Journal
Information Technology & Electrical Engineering

ISSN: - 2306-708X

A Symbol Scrambling and Limiting Approach to Improve the Selective Mapping Technique of PAPR Reduction in OFDM

[1] Mohammed Zakee Ahmed and [2] Sayyad Ajij Dildar

[1]Department of Electronics and Telecommunication Engineering, Assistant Professor, PICT Pune, India

[2]Department of Electronics and Telecommunication Engineering, Vice Principal, MIT Aurangabad, India

E-mail: [1]zakeeahmed@pict.edu, [2]ajij.sayyad@mit.asia

ABSTRACT

The Orthogonal Frequency Division Multiplexing (OFDM), the most well-known PHY technique can be seen in almost all types of networks right from a short distance Personal Area Network (PAN) to a Wide Area Network or Metropolitan Area Network (WAN or MAN). Despite tens of advantages, it has one severe disadvantage, the High Peak to Average Power Ratio, which simply means a wide gap in between average power and peaks of a time-domain OFDM signal. Selective Mapping (SLM) is a one of the identified prominent technique in PAPR reduction of OFDM. The major shortcoming of the SLM technique is high complexity in computation. To reduce further PAPR and to optimize the computational complexity, the present work, called *Symbol Scrambling and Limiting*, is presented. Here these issues are addressed by applying a reduced number of multiplications of input symbol and phase rotation vectors and applying amplitude limiting after that. With this approach, fewer multiplications have given reduced complexity of computation, and amplitude limiting has given more improved PAPR results. The OFDM signal is designed by following the PHY specifications of the IEEE WLAN 802.11anetwork standard using one of the state-of-the-art tools called LabVIEW.

Keywords: *OFDM, PAPR, SLM, LabVIEW, WLAN*

1. INTRODUCTION

1.1 OFDM

OFDM is a manner of modulation used for more traditional forms of digital data transmission. It utilizes many carriers called subcarriers, together to provide many advantages over plain modulation formats. OFDM can transmit the bulk of data over Radio waves, and it is one of the most known prominent multicarrier multiplexing accesses Technique. OFDM utilizes a frequency spectrum of almost 40-50% more than conventional FDM and has an excellent performance in the multipath fading channel. Figure 1 shows the basic principle of OFDM symbol formation is split of a frequency domain high-rate digitally modulation mapped data stream into several lower rate streams and transmitting them simultaneously on many these low-rate subcarriers by integrating them over a symbol period. These subcarriers are mutually orthogonal, which indicates a precise mathematical relationship amongst them, making them zero upon the cross product. If a replica image part of the symbol time-domain waveform is put at the start of the Symbol as the guard period, it effectively extends the length of the Symbol, while maintaining the orthogonality of the waveform. The guard period is then referred to as a cyclic prefix (CP). This concept is represented in Figure 1. Cyclic prefix helps the OFDM signal to deal with multipath effects in the channel [1-2].

Consider q OFDM symbol number each having N constellation point symbols, $X_{p,q} = [X_{0,q}, X_{1,q},\ldots, X_{N-1,q}]$ these are complex number symbols from a set of signal constellation points, $\{\Psi\}$, the OFDM signal can be represented with equation 1.

$$s_{r,q} = \frac{1}{\sqrt{N}} \sum_{p=0}^{N-1} X_{p,q} e^{j2\pi \frac{r}{N} p} \qquad \begin{matrix} 0 \le r \le N-1 \\ 0 \le p \le N-1 \end{matrix} \qquad (1)$$

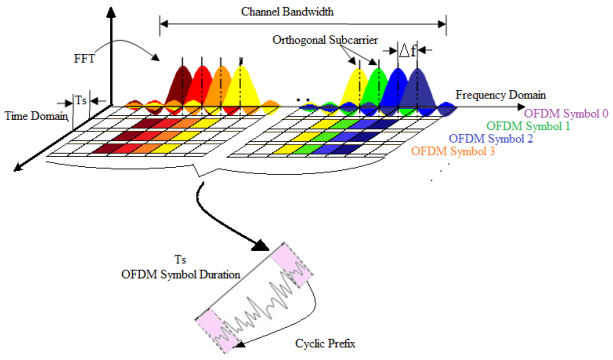

Figure-1: Basic principle of OFDM symbol formation

The $s_{r,q} = [s_{0,q}, s_{1,q},\ldots, s_{N-1,q}]$ are carrier amplitudes associated with the OFDM symbol, which is a formal expression for IFFT, $\mathfrak{F}^{-1}\{X_{p,q}\}$. Equation 2 depicts an infinite sequence of OFDM symbols to be transmitted.

$$s(t) = \sum_{q=-\infty}^{\infty} s_q(t) = \sum_{q=-\infty}^{\infty} \sum_{p=0}^{N-1} X_{p,q} \phi_p(t - qT) \qquad (2)$$

Volume 9, Issue 4
August 2020

ITEE Journal
Information Technology & Electrical Engineering

ISSN: - 2306-708X

1.2. PAPR

In an OFDM signal, several subcarriers get aligned together in the time domain; this may cause significant peaks or faded samples; this phenomenon is measured in terms of the difference between peak power and average power of the signal. Peak to Average Power Ratio (PAPR) or only Peak-to-Average Power (PAP) is used for measuring this effect in OFDM. PAPR can be defined with the ratio of Peak power to the average power of the signal. The PAPR is in general measure in dB with equation $PAPR_{dB} = 10\ log_{10}(PAPR)$ [1-2]. Mathematically it is defined as given in equation 3

$$\xi = \frac{\max\limits_{\forall\, q,r\in[0,N-1]} \left|s_{r,q}(t)\right|^2}{\mathrm{E}\left\{\left|s_{r,q}(t)\right|^2\right\}} \qquad (3)$$

2. RELATED WORK

Reducing PAPR in OFDM signal gives many advantages in developing transmitter-receiver of the communication systems. The advantages include the consumption of the least power and the least complexity in both hardware and software. For many decades there is continuous improvement in PAPR reduction technique [3]. From the recent studies, the CSLM is observed a prominent technique of PAPR reduction. This technique, too, had limitations of High Computational Complexity [4-6]. A simulation model developed in the LabVIEW development environment, following is the implementation details [7]. The CSLM requires a database of random phase rotation vectors BU, here 2D array-constant is used to store these vectors. The size of the input symbol is 64; hence the size of each BU is also 64. For pointwise multiplexing array indexing is used in the for-loop structure, so each value from both input symbol and 'uth 'B is multiplied with each other point by point [8-9]. The resultant Symbol is transformed with IFFT, and its PAPR is evaluated. The Symbol that is giving minimum PAPR will be nominated, and it is sent along with the index number 'u.' A specialized receiver is designed to decode the CSLM treated signal at the receiver side; it increases the complexity of the receiver [10]. The receiver must have precisely the same set of random phase vectors as that of the transmitter. At the receiver, the received signal has two parts first is the data symbol, and the second is the side information [11]. With side information first, the random phase vector is extracted from all its U copies. Then this random phase vectors are used to perform division operation with data symbol; the result of this division operation will be the original data symbol [12].

The authors of [3] have claimed the reduction of PAPR around 6.1 dB for 0.1% of P_r [PAPR>PAPR$_0$] by applying filtering post-SLM, the BER was very poor. The clipping ratio had derived from equation 4.

$$CR = 20log\left(\frac{C}{\sqrt{P_{avg}}}\right) \qquad (4)$$

[3] has used the IFFT multiple times, which has increased the computation. [4] has used the Hadamard Matrix to create phase rotation vectors and applied this technique in an optical fiber-based trans-receiver. [4] has claimed a reduction of PAPR around 7-9 dB for 0.1% of P_r [PAPR>PAPR$_0$]. For the generating of phase rotation vectors [5] utilizes Reed-Muller codes with a predefined order in two forms viz. natural and random with this [5] has claimed the reduction of PAPR more than 7 dB for 0.1% of P_r [PAPR>PAPR$_0$]. [6] proposed a phase optimization algorithm where the reduction of PAPR around 3 -6 dB for 0.1% of P_r [PAPR>PAPR$_0$] has been demonstrated. However, at the receiver side, what is the impact of these techniques on BER has not been demonstrated. [c] applied cyclic shift over scrambling and tested the results with max PAPR 7-8 dB for 0.1% of P_r [PAPR>PAPR$_0$]

3. PROPOSED DESIGN

The input frequency symbols $x = [x_0, x_1, x_2, \ldots x_{N-1}]$ pointwise multiplied with M different unique phase rotation factors $b_m = [b_m^0, b_m^1, b_m^2, \ldots b_m^{N-1}]$, these are designed least complex than CSLM techniques to address the computational complexity issue of the CSLM technique. This point multiplication is done along with IFFT, as shown in equation 4.

$$X_m^n = \sum_{n=0}^{N-1} x_n\, b_m^n e^{j\frac{2\pi nt}{N}} \qquad (4)$$

After this multiplication, the symbol set of minimum PAPR chosen with equation 5, the index number of phase rotation vector for which minimum PAPR is achieved, is referred to as side information as depicted with equation 6.

$$X_{SLM} = \arg\min_{m=0,1,2,..M-1} min_{X_m^n}\left(\max_{n=0,1,2,..N-1} |X_m^n|\right) \qquad (5)$$

$$\check{X} = \arg\min_{m=0,1,2,..M-1} min_m\left(\max_{n=0,1,2,..N-1} |X_m^n|\right) \qquad (6)$$

$$x_{SSL} = \begin{cases} x_{SLM} & |x_{SLM}| < A \\ Ae^{j\theta(t)} & |x_{SLM}| > A \end{cases} \qquad (7)$$

Now, from this time-domain signal, the peaks are controlled with amplitude limiting, as depicted in equation 7. According to [10], the unity amplitude complex phase rotation factors (b_m) can be used to avoid the complex multiplication operations, thus values of b_m are modified and used in the SSL technique. The overall process is as shown in Figure 2. Here the modified phase rotation vectors are referred to as unique phase vectors, and the resultant matrix of point multiplication is referred to as a scrambled symbol set. From this set, one original Symbol which has got scrambled samples due to unique-vector multiplication is selected based on the least PAPR. Moreover, the index no of unique-phase vector that gives the least PAPR is treated as side information. Additionally, the peak amplitude is limited to a threshold value. The threshold amplitude limiting will clip very few symbols as improved SLM will reduce the number of occurrences of peaks; this will give the benefit of clipping as well as scrambling.

Volume 9, Issue 4
August 2020

ITEE Journal
Information Technology & Electrical Engineering

ISSN: - 2306-708X

A Brief of precise PAPR measurement tool:

The reason for measuring the highest value of a peak is not the right way of PAPR measurement is as described in the following section with the justification of the right tool [13-14].

The PAPR equation in terms of the number of active subcarriers N_{used} and variance σ_x^2 can be expressed as in equation 8

$$\xi \leq N_{used} \frac{\max_{x\in\Psi}|X|^2}{\sigma_x^2} \quad (8)$$

When all the subcarriers have the same phase, the equality in equation 8 will achieve.

$$\arg\{x_{0,q}\} = \arg\{x_{0,q}\} \quad ; \forall p = 0,1,\dots,N-1. \quad (9)$$

From equation 8 and 9,

$$\xi = N_{used}\xi_{\Psi} \quad (10)$$

Where ξ_{Ψ} is the PAPR of input signal constellation Ψ

Let us say Ψ are M-QAM constellations

$$\max_{x\in\Psi}|X| = \begin{cases} \sqrt{2}\left(\sqrt{M}-1\right) & n \text{ is even} \\ \sqrt{M+2} & n \text{ is odd} \end{cases} \quad (11)$$

Where, $M = 2^n$, n being several bits per subcarrier.

The variance of M-QAM is

$$\sigma_x^2 = 2\,(M-1)/3 \quad (12)$$

After analyzing equation 10,11 and 12, the PAPR of M-QAM-OFDM can be written as

$$\xi_{\max} = \begin{cases} 3N_{used}\dfrac{\sqrt{M}-1}{\sqrt{M}+1} & n \text{ is even} \\ 1.5N_{used}\dfrac{M+2}{M-1} & n \text{ is odd} \end{cases} \quad (13)$$

With WLAN standard IEEE 802.11a of Wi-Fi following test cases can be applied to equation 13.

Case 1:

For the Modulation Scheme BPSK, the equation 13 leads $\xi_{\max}$ with N_{used}=48 as follows

$$\xi_{\max} = 3X48X\,\frac{\sqrt{2}-1}{\sqrt{2}+1} = 24.7$$

Now,

$$PAPR_{dB} = 10\,log_{10}(\xi_{max}) = 10.\log 24.7$$

Thus,

$$PAPR_{dB(BPSK)} = 13.93dB \quad (14)$$

Case 2:

Similar to BPSK, Modulation Scheme =4-QAM,

$$\xi_{\max} = 96$$
$$PAPR_{dB} = 10.log_{10}(96)$$

Thus,

$$PAPR_{dB(4-QAM)} = 19.82dB \quad (15)$$

Case 3:

Modulation Scheme =16-QAM,

$$\xi_{\max} = 86.4$$
$$PAPR_{dB} = 10.\log 86.4$$

Thus,

$$PAPR_{dB(16-QAM)} = 19.37dB \quad (16)$$

Case 4:

Modulation Scheme =64-QAM,

$$\xi_{\max} = 140$$
$$PAPR_{dB} = 10.log_{10}\,140$$

Thus,

$$PAPR_{dB(64-QAM)} = 21.45dB \quad (17)$$

The equation 14, 15, 16, and 17 shows maximum PAPR for modulation BPSK, 4-QAM, 16-QAM, and 64-QAM, respectively. The probability of occurrence of theoretical maximum PAPR for $M = 4$, which leads a maximum 16 patterns is $16/4N_{used}$. That is, the probability of the occurrence of theoretical PAPR is significantly less. *Hence the upper bound cannot be said to be a useful tool for analysis of the PAPR of a given OFDM signals and its statistical distribution.*

The transmitted signal becomes intimately involved in Gaussian distribution, according to the central limit theorem (CLT). Also, the amplitude of the OFDM signal has a Rayleigh distribution. Consider ξ_0 PAPR threshold and $\Pr\{\xi_0\}$ Probability of exceedance. $e^{-\xi_0}$ The probability that a single sample per unit time that exceeds the threshold ξ_0. In a time-domain OFDM signal the probability that the magnitude of a single signal sample not to exceed a certain amplitude threshold $s_0 > 0$, illustrated in equation 18.

$$\Pr\{|s_{r,q}| < s_0\} = 1 - exp\left(-\frac{s_0^2}{\sigma_s^2}\right) \quad (18)$$

With the consideration that the samples are statistically independent, the probability of exceedance of at least one magnitude of the entire OFDM symbol to a given threshold given with equation 19.

$$\Pr\left\{\max_{q\in[0,N-1]}|s_{r,q}| \geq s_0\right\} = 1 - \left(1 - \exp\left(-\frac{s_0^2}{\sigma_s^2}\right)\right)^N \quad (19)$$

Thus the equation 19 yields the useful tool of analyzing the PAPR

$$\Pr\{\xi \geq \xi_0\} = 1 - \left(1 - e^{-\xi_0}\right)^N \quad (20)$$

Equation 20 depicts the *Complementary Cumulative Distribution Function* that is (CCDF), which is a recognized tool for performance measure for PAPR in OFDM signal. It signifies the probability of exceeding PAPR of a data block to an absolute threshold value. For a vast number of subcarriers with the uncorrelated input data. The effect of frame structure on signal deterioration due to channel, here AWGN, can be analyzed with Bit Error Ratio Vs. The ratio of Energy/Bit (E_b) to the Spectral Noise Density (N_0) in short BER vs. E_b/N_0 [13-14]. Figure 3 shows the LabVIEW Module-specific to SSL, which is one of the parts of the trans-receiver simulation module developed for present work.

Volume 9, Issue 4
August 2020

ITEE Journal
Information Technology & Electrical Engineering

ISSN: - 2306-708X

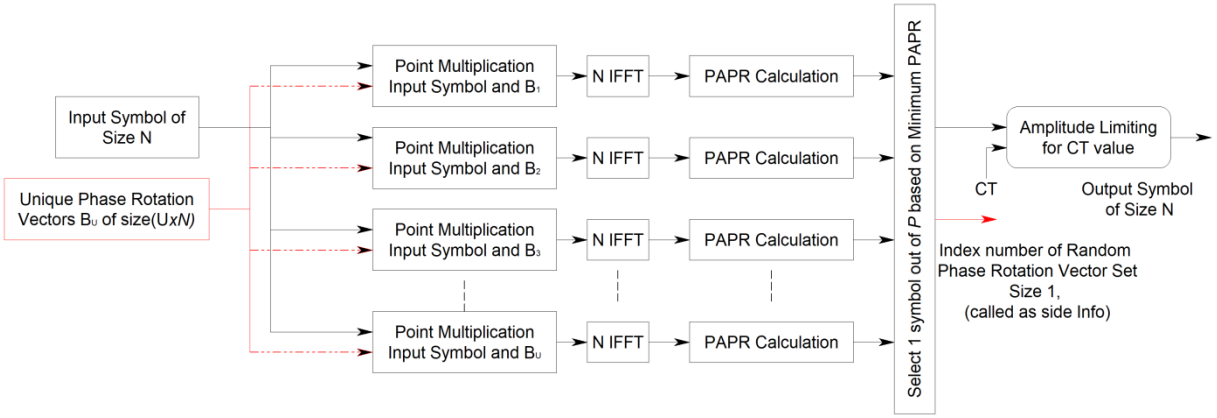

Figure-2: Block representation of SSL Technique

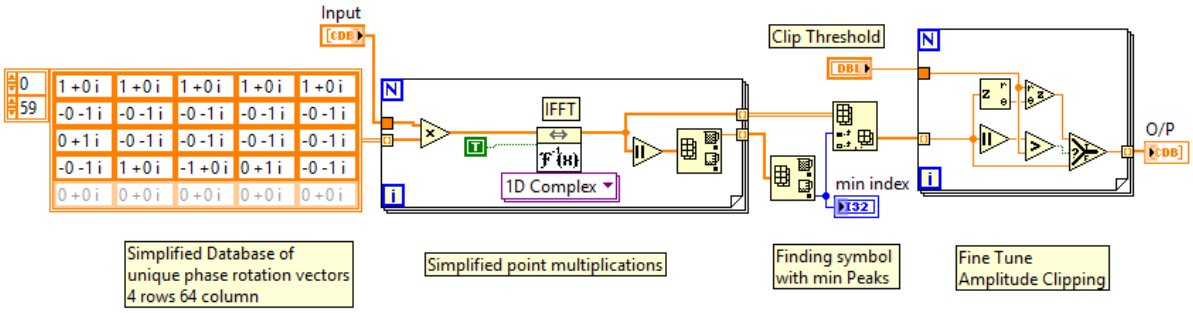

Figure-3: LabVIEW module of SSL technique

Other than this module, the simulation model has decoder of SSL, modules of PN sequence generator, symbol mapping and de mapper of BPSK, 4-QAM, 16-QAM, and 64-QAM, OFDM framework including CP insertion removal, zero-padding insertion, and removal. Along with this measurement tools CCDF and BER vs. Eb/N0 module. All these modules integratively from a simulation model of OFDM Transceiver. Figure 4 shows the flow chart of both transmitter and receiver of the SSL Technique.

Flow Chart

The figure 4 (a) shows the step by step signal construction illustrated in the form of a flow chart, where the pointwise multiplication of unique phase rotation vectors with input symbol, and shortlisting the symbol copy having least PAPR from all copies of input scrambled Symbol is illustrated. This illustration has a more simplified description given in the algorithm of the transmitter, as in the following section.

Figure 4 (b) is the flow chart to be deployed at the receiver to decode the transmitted signal by dividing the same set of phase rotation vectors, which is extracted from the database followed by received side information.

Algorithm

Transmitter

i. Start
ii. Take U random phase vectors set B, each of size N
iii. Take a Symbol of N size
iv. Perform pointwise multiplication of each u^{th} value of B, and input symbol
v. Perform IFFT on each of the Resultant Symbol and Measure the PAPR
vi. Choose one Symbol out of resultant symbols based on minimum PAPR
vii. Perform Fine Amplitude Clipping on Selected Symbol
viii. Send the selected Symbol with its index number
ix. Stop

Receiver:

i. Start
ii. Separate side-information and data symbol from the received information
iii. Perform FFT on data symbol
iv. Use the side-information index number, to extract the corresponding row from phase rotation vector matrix
v. Use this row and divide the data symbol with it
vi. Collect the resultant Symbol which is the original Symbol
vii. stop

Volume 9, Issue 4
August 2020

ITEE Journal
Information Technology & Electrical Engineering

ISSN: - 2306-708X

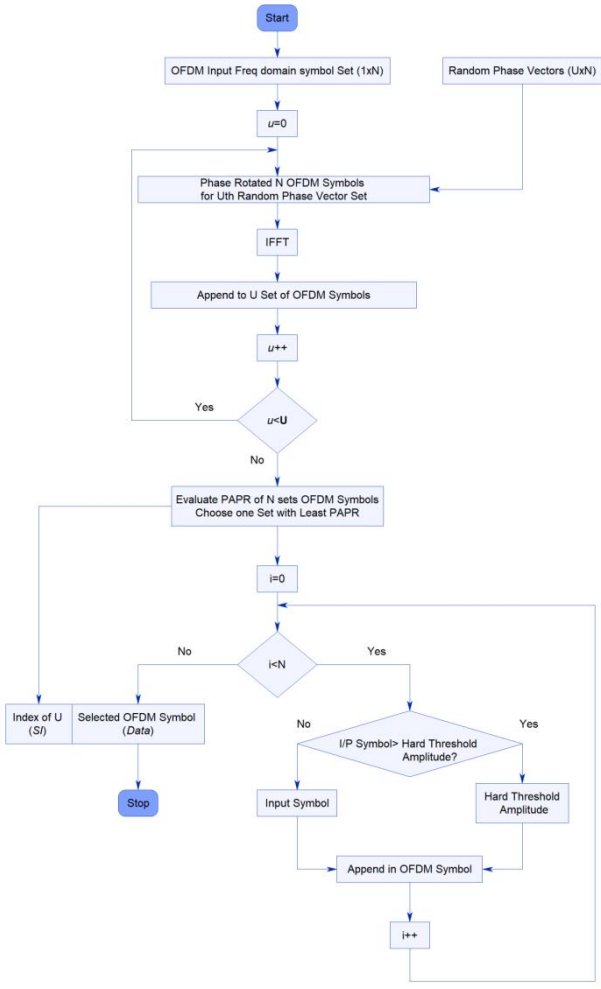

(a)

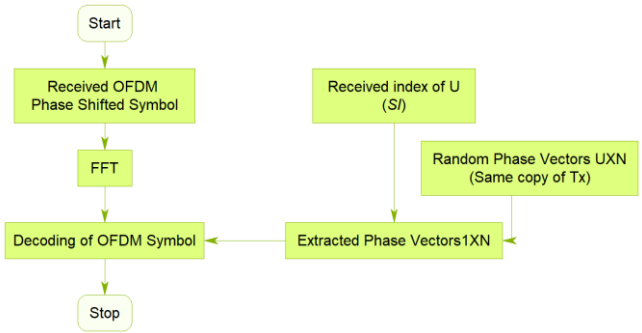

(b)

Figure-4: Flow chart (a) Tx (b) Rx of SSL Technique

4. RESULTS AND DISCUSSIONS

SSL is evaluated with CSLM, and original OFDM signal without any scheme applied. The evaluation is made in terms of CCDF and BER vs. E_b/N_0.

Figure 5 (a) depicts CCDF for BPSK Modulation; here, SSL covers the region up to 5.2 dB, which shows a perfect improvement in PAPR. In figure 5 (b), the BER vs. E_b/N_0 of SSL is even better than CSLM showing the least region belongs to error symbols.

Figure 6 depicts (a) CCDF (b) BER vs. E_b/N_0 for 4-QAM Modulation here; also, the improvement in CCDF is observed. BER performance is similar to CSLM and better than the actual OFDM signal with no PAPR reduction scheme applied.

Figure 7 depicts (a) CCDF (b) BER vs. E_b/N_0 for 16-QAM Modulation. Here the CCDF is approx the same as that of CSLM, but the BER performance is improved.

Figure 8 depicts (a) CCDF (b) BER vs. E_b/N_0 for 64-QAM Modulation. CCDF of SSL is improved over CSLM and signal with no scheme, and the BER performance is similar to CSLM with no degradation.

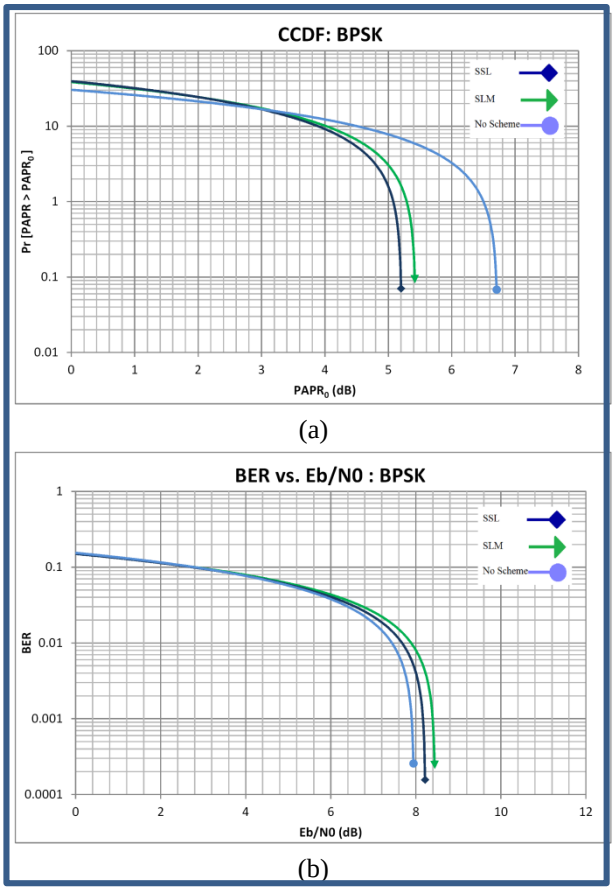

(a)

(b)

Figure-5: (a) CCDF (b) BER vs. Eb/N0 for BPSK

Volume 9, Issue 4
August 2020

ITEE Journal
Information Technology & Electrical Engineering

ISSN: - 2306-708X

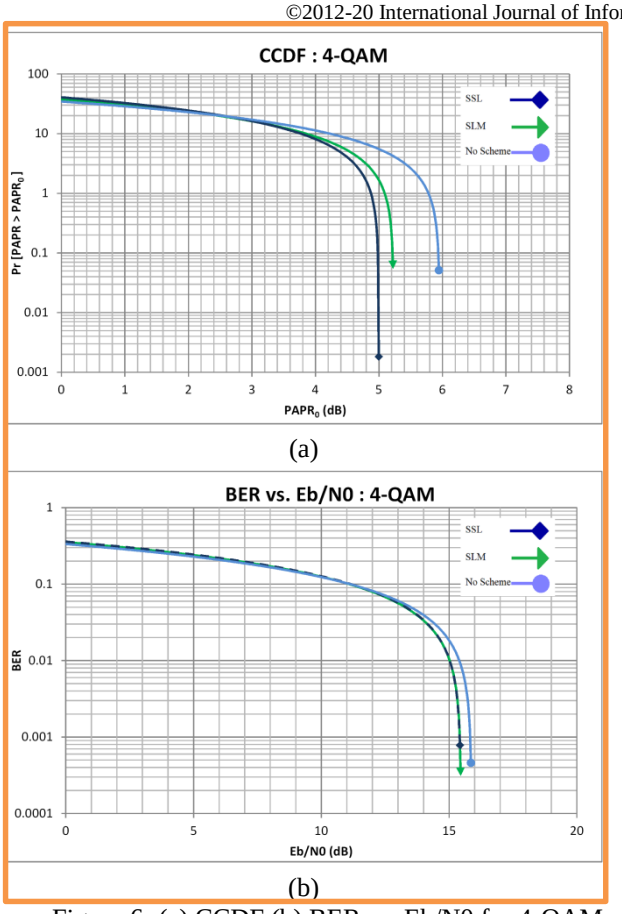

Figure-6: (a) CCDF (b) BER vs. Eb/N0 for 4-QAM

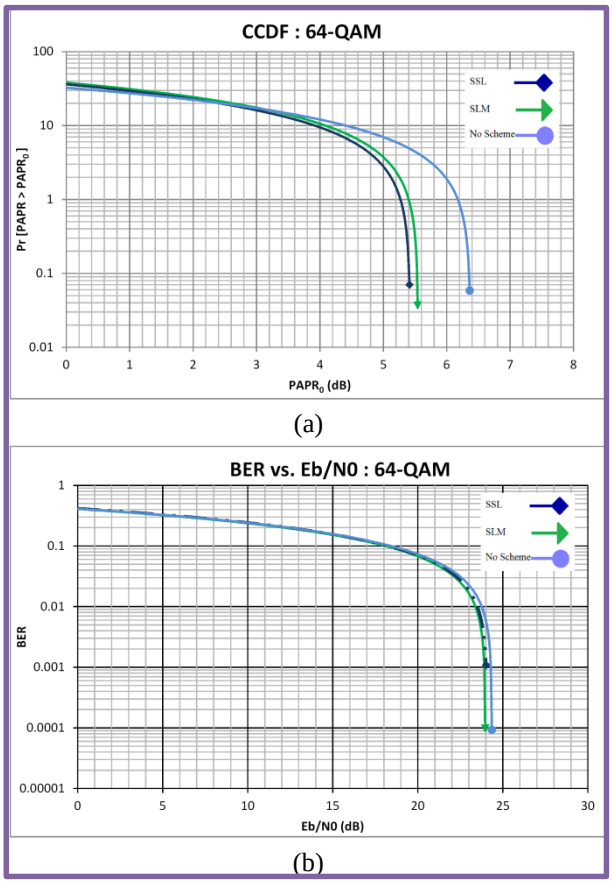

Figure-8: (a) CCDF (b) BER vs. Eb/N0 for 64-QAM

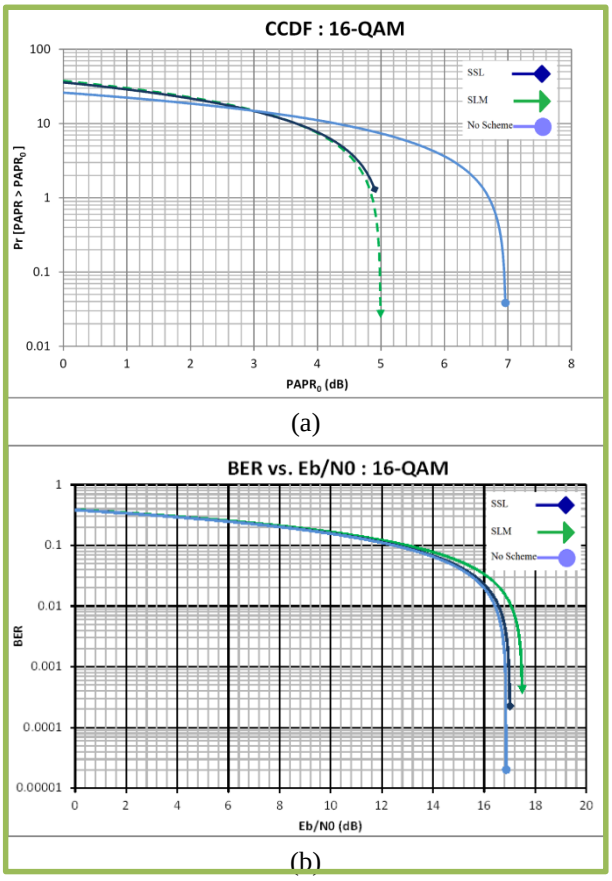

Figure-7: (a) CCDF (b) BER vs. Eb/N0 for 16-QAM

5. CONCLUSION

In the present manuscript, we have demonstrated the detailed description of the PAPR reduction technique of the OFDM signal; we named it Symbol Scrambling and Limiting technique. The SSL technique is the improvement over the Conventional Selective Mapping Technique concerning its CCDF performance, BER performance, and Computational complexity. Various experimentations performed for getting the phase rotation vector set that takes least multiplications and work upon more improvement in PAPR along with this amplitude limiting is added at the end of signal design to control higher peaks. This way assures zero peaks above threshold also sustains the BER performance with the least data loss.

The signal design and testing followed the 802.11a frame structure. LabVIEW development platform is used for overall signal designed; thoroughly both transmitter and receiver are designed. In the present manuscript, the module of the PAPR reduction module is illustrated and explained thoroughly in support of the flow chart and algorithm. The present technique has given an excellent improvement in both CCDF and BER performances, and thus it may be followed in other OFDM standards as well. Thus the problem of HPA going in saturation region can be fully addressed with this technique with controlled computational complexity and data loss.

6. ACKNOWLEDGMENT

We would like to present a sincere gratitude to Management PICT, Dr. P.T. Kulkarni Principal PICT and Dr. S. V. Gaikwad HoED PICT for providing access to laboratories and resources also for their continuous motivation and support.

REFERENCES

[1] G. Misra, A. Agarwal, and K. Agarwal, "A technological analysis and survey on peak-to-average power reduction (PAPR) in MIMO-OFDM wireless system," ***2016*** *International Conference on Electrical, Electronics, and Optimization Techniques (ICEEOT)*, Chennai, 2016

[2] U. B. Mahadevaswamy and M. N. Geetha, "A comparative survey on PAPR reduction in OFDM signal," ***2016*** *(ICEECCOT)*, Mysuru, 2016

[3] A. Cuenin and N. Engin, "Selective clipping and filtering: A low-EVM PAPR reduction scheme for OFDM standards," ***2016*** *IEEE 27th Annual International Symposium on (PIMRC)*, Valencia, 2016

[4] M. I. Al-Rayif, H. Seleem, A. Ragheb, and S. Alshebeili, "A Novel Iterative-SLM Algorithm for PAPR Reduction in 5G Mobile Fronthaul Architecture," in *IEEE Photonics Journal*, vol. 11, no. 1, pp. 1-12, Feb. **2019**

[5] H. Liang, "Selective Mapping Technique Based on an Adaptive Phase-Generation Mechanism to Reduce Peak-to-Average Power Ratio in Orthogonal Frequency Division Multiplexing Systems," in *IEEE Access*, vol. 7, pp. 96712-96718, **2019**

[6] M. N. Mohammed, A. K. Nahar, A. N. Abdalla and O. A. Hammood, "Peak-to-average power ratio reduction based on optimized phase shift technique," ***2017*** *17th ISCIT*, Cairns, QLD, 2017

[7] P. Dewi Pamungkasari and Y. Sanada, "Time-domain cyclic-selective mapping for PAPR reduction using delayed correlation with a matched filter in an OFDM system," *2015 22nd (ICT)*, Sydney, NSW, **2015**

[8] W. A. Syafei, A. Hidayatno, and A. A. Zahra Macrina, "Backward Compatible Low PAPR Preamble for Very High Throughput WLAN IEEE802.11ac," *2019 6th ICITACEE*, Semarang, Indonesia, **2019**

[9] F. Sandoval, G. Poitau, and F. Gagnon, "Hybrid Peak-to-Average Power Ratio Reduction Techniques: Review and Performance Comparison," in *IEEE Access*, vol. 5, pp. 27145-27161, **2017**

[10] Y. A. Jawhar *et al.*, "A Review of Partial Transmit Sequence for PAPR Reduction in the OFDM Systems," in *IEEE Access*, vol. 7, pp. 18021-18041, **2019**

[11] S. Mishra and A. Agarwal, "Peak to average power ratio reduction in sub-carrier Index modulated OFDM using selective mapping," *2017 International Conference on Computer, Communications and Electronics (Comptelix)*, Jaipur, **2017**

[12] M. S. Ahmed, S. Boussakta, A. Al-Dweik, B. Sharif, and C. C. Tsimenidis, "Efficient Design of Selective Mapping and Partial Transmit Sequence Using T-OFDM," in *IEEE Transactions on Vehicular Technology*, vol. 69, no. 3, pp. 2636-2648, March **2020**

[13] A. Tripathi, V. Anand, and A. K. Jain, "Study of OFDM and analysis of BER using intercarrier interference technique," ***2016*** *ICICCS-INBUSH*, Noida, **2016**

[14] S. Ramavath, B. Ramavath, and R. Akhil, "Theoretical Analysis of the PAPR for DFT Spreading Based FBMC," *2019 4th International Conference on RTEICT*, Bangalore, India, **2019**

AUTHOR PROFILES

Mohammed Zakee Ahmed completed his M-Tech from National Institute of Electronics & Information Technology (NIELIT),(erstwhile DOEACC Society), an Autonomous Scientific Society, under the admin of Ministry of Electronics & Information Technology (MoE&IT), Government of India, has Ten years of experience in Engineering Education, Research and Consultant. He is presently designated as an Assistant professor in the Department of Electronics and Telecommunication Engineering at Pune Institute of Computer Technology Pune.

Dr. Sayyad Ajij has completed his Ph.D. (Systems and Control Engineering) from IIT Bombay Mumbai, has 14 years of Engineering Education and research experience. Currently, he is working as Associate Professor, and Vice-Principal (Academics) at Marathwada Institute Of Technology, Aurangabad his Area of Specialization is Signal Processing, Robotics and Process Control.